

## Role of Sequence in Salt-Bridge Formation for Alkali Metal Cationized GlyArg and ArgGly Investigated with IRMPD Spectroscopy and Theory

James S. Prell,<sup>†</sup> Maria Demireva,<sup>†</sup> Jos Oomens,<sup>‡</sup> and Evan R. Williams<sup>\*†</sup>

*Department of Chemistry, University of California, Berkeley, California 94720-1460, and FOM Institute for Plasma Physics "Rijnhuizen," Edisonbaan 14, 3439 MN Nieuwegein, The Netherlands*

Received October 16, 2008; E-mail: williams@cchem.berkeley.edu

**Abstract:** The roles of hydrogen bonding, electrostatic interactions, sequence, gas-phase basicity, and molecular geometry in determining the structures of protonated and alkali metal-cationized glyceryl-L-arginine (GlyArg) and L-arginylglycine (ArgGly) were investigated using infrared multiple photon dissociation spectroscopy in the spectral range 900–1800 cm<sup>-1</sup> and theory. The IRMPD spectra clearly indicate that GlyArg•M<sup>+</sup>, M = Li, Na, and Cs, form similar salt-bridge (SB) structures that do not depend significantly on metal ion size. In striking contrast, ArgGly•Li<sup>+</sup> exists in a charge-solvated (CS) form, whereas ArgGly•M<sup>+</sup>, M = K and Cs, form SB structures. SB and CS structures are similarly populated for ArgGly•Na<sup>+</sup>. Computed energies of low-energy structures are consistent with these results deduced from the experimental spectra. By comparison to Arg•M<sup>+</sup>, GlyArg•M<sup>+</sup> and ArgGly•M<sup>+</sup> have a greater and lesser propensity, respectively, to form SB structures. The greater propensity for GlyArg to adopt SB structures in complexes with smaller metal cations than for ArgGly is due to the ability of alkali metal-cationized GlyArg to adopt a nearly linear arrangement of formal charge sites, a structure unfavorable for ArgGly complexes due to geometric constraints induced by its different amino acid sequence. The amide carbonyl oxygen solvates charge in both the SB and CS form of both dipeptides. ArgGly is calculated to be slightly more basic than GlyArg, indicating that differences in intrinsic basicity do not play a role in the relative SB stabilization of these ions. Loss of a neutral water molecule from complexes in which SB structures are most stable indicates that CS structures are intermediates in the dissociation pathway, but these intermediates do not contribute to the measured IRMPD spectra.

### Introduction

Electrostatic interactions and hydrogen bonding are important in molecular structure and reactivity. Ionic interactions, whether from charged functional groups, metal ions, or counterions, can either stabilize or destabilize protein conformations and play a major role in protein–substrate<sup>1</sup> and protein–protein<sup>2</sup> interactions. Metal ion specific noncovalent interactions have been implicated in the selectivity of ion channels,<sup>3</sup> and metal ions are required for the activity of many proteins.<sup>4</sup> Solvent can significantly influence electrostatic interactions as well as intramolecular hydrogen bonding.<sup>5</sup> Information about the intrinsic effects of hydrogen bonding and electrostatic interactions on biomolecule structure can be obtained from gas-phase experiments, and, in principle, the role solvent plays in hydrogen bonding and electrostatic interactions can be inferred from these studies.

Structures of protonated and cationized amino acids have been extensively investigated using a variety of gas-phase methods,<sup>6–50</sup> and these studies provide excellent comparisons to those done

<sup>†</sup> University of California, Berkeley.

<sup>‡</sup> FOM Institute for Plasma Physics "Rijnhuizen".

- (1) Garcia-Viloca, M.; Gao, J.; Karplus, M.; Truhlar, D. G. *Science* **2004**, *303*, 186–195.
- (2) Schreiber, G.; Fersht, A. R. *Nat. Struct. Biol.* **1996**, *3*, 427–431.
- (3) Dougherty, D. A. *Science* **1996**, *271*, 163–168.
- (4) Vogel, H. J. *Biochem. Cell Biol.* **1994**, *72*, 357–376.
- (5) Patriksson, A.; Adams, C. M.; Kjeldsen, F.; Zubarev, R. A.; van der Spoel, D. *J. Phys. Chem. B* **2007**, *111*, 13147–13150.

- (6) Lemoff, A. S.; Bush, M. F.; Williams, E. R. *J. Am. Chem. Soc.* **2003**, *125*, 13576–13584.
- (7) Wyttenbach, T.; Witt, M.; Bowers, M. T. *J. Am. Chem. Soc.* **2000**, *122*, 3458–3464.
- (8) Constantino, E.; Rodriguez-Santiago, L.; Sodupe, M.; Tortajada, J. J. *Phys. Chem. A* **2005**, *109*, 224–230.
- (9) Cox, H. A.; Julian, R. R.; Lee, S. W.; Beauchamp, J. L. *J. Am. Chem. Soc.* **2004**, *126*, 6485–6490.
- (10) Bush, M. F.; Oomens, J.; Saykally, R. J.; Williams, E. R. *J. Am. Chem. Soc.* **2008**, *130*, 6463–6471.
- (11) Dunbar, R. C.; Polfer, N. C.; Oomens, J. *J. Am. Chem. Soc.* **2007**, *129*, 14562–14563.
- (12) Kapota, C.; Lemaire, J.; Maitre, P.; Ohanessian, G. *J. Am. Chem. Soc.* **2004**, *126*, 1836–1842.
- (13) Polfer, N. C.; Oomens, J.; Dunbar, R. C. *Phys. Chem. Chem. Phys.* **2006**, *8*, 2744–2751.
- (14) Polfer, N. C.; Paizs, B.; Snoek, L. C.; Compagnon, I.; Suhai, S.; Meijer, G.; von Helden, G.; Oomens, J. *J. Am. Chem. Soc.* **2005**, *127*, 8571–8579.
- (15) Polfer, N. C.; Oomens, J.; Moore, D. T.; von Helden, G.; Meijer, G.; Dunbar, R. C. *J. Am. Chem. Soc.* **2006**, *128*, 517–525.
- (16) Bush, M. F.; Forbes, M. W.; Jockusch, R. A.; Oomens, J.; Polfer, N. C.; Saykally, R. J.; Williams, E. R. *J. Phys. Chem. A* **2007**, *111*, 7753–7760.
- (17) O'Brien, J. T.; Prell, J. S.; Steill, J. D.; Oomens, J.; Williams, E. R. *J. Phys. Chem. A* **2008**, *112*, 10823–10830.
- (18) Bush, M. F.; Oomens, J.; Saykally, R. J.; Williams, E. R. *J. Phys. Chem. A* **2008**, *112*, 8578–8584.

in the condensed phase. For example, the nonzwitterionic forms of the 20 common  $\alpha$ -amino acids are more stable in the gas phase than their zwitterionic forms. However, gas-phase complexes of amino acids with metal cations can exist in either charge-solvated (CS) forms, where the metal is chelated by formally neutral heteroatoms, or salt-bridge (SB) forms in which the metal ion is coordinated to the zwitterionic form of the amino acid. For cationized aliphatic amino acids, the CS form is more stable, but the stability of the SB form increases with increasing proton affinity.<sup>6,7</sup> In contrast, this relationship is much less direct for amino acids with sidechains containing heteroatoms.<sup>16–23</sup> Arginine, the most basic of the common  $\alpha$ -amino acids, is particularly interesting because the stabilities of the SB and CS

forms are similar, and which form is lower in energy depends on cation size.<sup>21,22,33–35</sup> The CS form is more stable when lithiated, but the SB form is more stable for potassium and larger cations. For sodium, the SB form is more stable, but a small fraction of CS population is also observed,<sup>21,22</sup> indicating that these two forms of the complex are very similar in energy.

Infrared multiple photon dissociation (IRMPD) spectroscopy has emerged as a powerful method that can provide detailed information about structures of gas-phase ions. Radiation from either free electron lasers or from tabletop OPO/OPA lasers has been used to investigate the structures of many cationized amino acids in the spectral range from 500–2000<sup>10–21</sup> and 2500–4000  $\text{cm}^{-1}$ ,<sup>22–25</sup> respectively. From these studies, it was found that the SB form of sodiated proline is more stable than the CS form,<sup>12</sup> but CS forms of alkali metal-cationized glycine,<sup>12</sup> tryptophan,<sup>13</sup> phenylalanine,<sup>14,24</sup> lysine,<sup>16</sup> glutamic and aspartic acid,<sup>17</sup> glutamine,<sup>18</sup> serine,<sup>19</sup> and threonine<sup>20</sup> are more stable. Evidence for a minor population of SB structures for cesiated serine has been reported.<sup>19</sup> Results from these studies indicate that for metal-cationized amino acids with heteroatom-containing sidechains, solvation of the charge by several polar functional groups in the CS form can effectively compete with the strong dipole stabilization possible in the SB form. Hydrogen bonding can contribute to the stability of either form.

In contrast to studies of individual amino acids, very few IRMPD studies have been conducted on metal-cationized peptides,<sup>14,51</sup> for which effects of charge solvation by the peptide backbone, sequence, or conformational effects may be significant. IRMPD studies of potassiated AlaPhe and PheAla show that these ions exist in a CS form where the amide carbonyl oxygen atom coordinates to the metal cation, and both the carboxylic acid carbonyl oxygen and the N-terminal nitrogen compete to solvate the charge.<sup>51</sup> As observed for potassiated phenylalanine,<sup>14</sup> the aromatic ring participates in solvating the metal cation in these two dipeptides. The IRMPD spectrum of potassiated Leu-enkephalin (Tyr-Gly-Gly-Phe-Leu), a pentapeptide with no basic residues, indicates that it forms a CS complex in which the charge is solvated primarily by amide carbonyl oxygen atoms.<sup>14</sup> The phenylalanine side chain does not interact with the charge due to steric hindrance. By comparison, potassiated bradykinin fragment 1–5 (Arg-Pro-Pro-Gly-Phe) exists as a SB complex in which the charge is solvated primarily by the amide carbonyl oxygen atoms, and the protonated side chain of the N-terminal arginine residue interacts with the C-terminal carboxylate group.<sup>14</sup> These and other studies,<sup>9,52–67</sup> including IRMPD of protonated peptides,<sup>56–61</sup> clearly show that charge solvation by amide groups, as well as the identity and location along the peptide backbone of constituent amino acid residues, are important factors in the structures of cationized peptides.

Because the CS and SB forms of metal-cationized arginine are close in energy, and the lowest-energy form depends on metal ion size, arginine-containing dipeptides are particularly

- (19) Armentrout, P. B.; Rodgers, M. T.; Oomens, J.; Steill, J. D. *J. Phys. Chem. A* **2008**, *112*, 2248–2257.
- (20) Rodgers, M. T.; Armentrout, P. B.; Oomens, J.; Steill, J. D. *J. Phys. Chem. A* **2008**, *112*, 2258–2267.
- (21) Forbes, M. W.; Bush, M. F.; Polfer, N. C.; Oomens, J.; Dunbar, R. C.; Williams, E. R.; Jockusch, R. A. *J. Phys. Chem. A* **2007**, *111*, 11759–11770.
- (22) Bush, M. F.; O'Brien, J. T.; Prell, J. S.; Saykally, R. J.; Williams, E. R. *J. Am. Chem. Soc.* **2007**, *129*, 1612–1622.
- (23) Bush, M. F.; Prell, J. S.; Saykally, R. J.; Williams, E. R. *J. Am. Chem. Soc.* **2007**, *129*, 13544–13553.
- (24) Stearns, J. A.; Mercier, S.; Seaiby, C.; Guidi, M.; Boyarkin, O. V.; Rizzo, T. R. *J. Am. Chem. Soc.* **2007**, *129*, 11814–11820.
- (25) Kamariotis, A.; Boyarkin, O. V.; Mercier, S. R.; Beck, R. D.; Bush, M. F.; Williams, E. R.; Rizzo, T. R. *J. Am. Chem. Soc.* **2006**, *128*, 905–916.
- (26) Oh, H. B.; Lin, C.; Hwang, H. Y.; Zhai, H. L.; Breuker, K.; Zabrouskov, V.; Carpenter, B. K.; McLafferty, F. W. *J. Am. Chem. Soc.* **2005**, *127*, 4076–4083.
- (27) Heaton, A. L.; Armentrout, P. B. *J. Phys. Chem. B* **2008**, *112*, 12056–12065.
- (28) Heaton, A. L.; Moision, R. M.; Armentrout, P. B. *J. Phys. Chem. A* **2008**, *112*, 3319–3327.
- (29) Hoyau, S.; Ohanessian, G. *Chem.—Eur. J.* **1998**, *4*, 1561–1569.
- (30) Hoyau, S.; Pelicier, J. P.; Rogalewicz, F.; Hoppilliard, Y.; Ohanessian, G. *Eur. J. Mass Spectrom.* **2001**, *7*, 303–311.
- (31) Jockusch, R. A.; Lemoff, A. S.; Williams, E. R. *J. Am. Chem. Soc.* **2001**, *123*, 12255–12265.
- (32) Jockusch, R. A.; Lemoff, A. S.; Williams, E. R. *J. Phys. Chem. A* **2001**, *105*, 10929–10942.
- (33) Jockusch, R. A.; Price, W. D.; Williams, E. R. *J. Phys. Chem. A* **1999**, *103*, 9266–9274.
- (34) Cerda, B. A.; Wesdemiotis, C. *Analyst* **2000**, *125*, 657–660.
- (35) Remko, M.; Fitz, D.; Rode, B. M. *J. Phys. Chem. A* **2008**, *112*, 7652–7661.
- (36) Kong, X. L.; Tsai, I. A.; Sabu, S.; Han, C. C.; Lee, Y. T.; Chang, H. C.; Tu, S. Y.; Kung, A. H.; Wu, C. C. *Angew. Chem., Int. Ed.* **2006**, *45*, 4130–4134.
- (37) Lemoff, A. S.; Bush, M. F.; O'Brien, J. T.; Williams, E. R. *J. Phys. Chem. A* **2006**, *110*, 8433–8442.
- (38) Lemoff, A. S.; Bush, M. F.; Williams, E. R. *J. Phys. Chem. A* **2005**, *109*, 1903–1910.
- (39) Lemoff, A. S.; Bush, M. F.; Wu, C. C.; Williams, E. R. *J. Am. Chem. Soc.* **2005**, *127*, 10276–10286.
- (40) Lemoff, A. S.; Williams, E. R. *J. Am. Soc. Mass Spectrom.* **2004**, *15*, 1014–1024.
- (41) Lemoff, A. S.; Wu, C. C.; Bush, M. F.; Williams, E. R. *J. Phys. Chem. A* **2006**, *110*, 3662–3669.
- (42) Rajabi, K.; Fridgen, T. D. *J. Phys. Chem. A* **2008**, *112*, 23–30.
- (43) Rak, J.; Skurski, P.; Simons, J.; Gutowski, M. *J. Am. Chem. Soc.* **2001**, *123*, 11695–11707.
- (44) Remko, M.; Rode, B. M. *J. Phys. Chem. A* **2006**, *110*, 1960–1967.
- (45) Rodgers, M. T.; Armentrout, P. B. *Acc. Chem. Res.* **2004**, *37*, 989–998.
- (46) Ruan, C. H.; Rodgers, M. T. *J. Am. Chem. Soc.* **2004**, *126*, 14600–14610.
- (47) Strittmatter, E. F.; Lemoff, A. S.; Williams, E. R. *J. Phys. Chem. A* **2000**, *104*, 9793–9796.
- (48) Talley, J. M.; Cerda, B. A.; Ohanessian, G.; Wesdemiotis, C. *Chem.—Eur. J.* **2002**, *8*, 1377–1388.
- (49) Wu, R. H.; McMahon, T. B. *J. Am. Chem. Soc.* **2007**, *129*, 4864–4865.
- (50) Wytenbach, T.; Witt, M.; Bowers, M. T. *Int. J. Mass Spectrom.* **1999**, *182–183*, 243–252.

- (51) Polfer, N. C.; Oomens, J.; Dunbar, R. C. *ChemPhysChem* **2008**, *9*, 579–589.
- (52) Abirami, S.; Wong, C. H. S.; Tsang, C. W.; Ma, N. L.; Goh, N. K. *J. Mol. Struct. (THEOCHEM)* **2005**, *729*, 193–202.
- (53) Lucas, B.; Grégoire, G.; Lemaire, J.; Maitre, P.; Ortega, J. M.; Rupenyán, A.; Reimann, B.; Schermann, J. P.; Desfrancois, C. *Phys. Chem. Chem. Phys.* **2004**, *6*, 2659–2663.
- (54) Cerda, B. A.; Hoyau, S.; Ohanessian, G.; Wesdemiotis, C. *J. Am. Chem. Soc.* **1998**, *120*, 2437–2448.
- (55) Kapota, C.; Ohanessian, G. *Phys. Chem. Chem. Phys.* **2005**, *7*, 3744–3755.

interesting to investigate to determine how sequence and higher-order structure influence the relative importance of electrostatic interactions and hydrogen bonding. Attachment of just a single water molecule to lithiated arginine, which has a CS structure,<sup>21,22</sup> can result in the SB form being more stable,<sup>23</sup> illustrating the delicate balance between the stabilities of these two forms of arginine. Here, results both from IRMPD spectroscopy over the spectral range 900–1800 cm<sup>-1</sup> and from computational chemistry of neutral, protonated, and alkali metal-cationized ArgGly and GlyArg are presented. These results show that the order of the two amino acids in these dipeptides has a significant influence on whether the CS or SB form of the cationized species is most stable and demonstrate that molecular geometry plays a critical role in stabilizing SB structures.

## Experimental Section

**IRMPD Spectroscopy.** IRMPD spectra were obtained using a 4.7 T Fourier-transform ion cyclotron resonance mass spectrometer coupled with a free electron laser (FELIX), which generates tunable IR radiation. A detailed description of the instrument<sup>68</sup> and experimental methods<sup>15</sup> can be found elsewhere. 60/40 water/methanol solutions containing GlyArg or ArgGly (Bachem Distribution Services, GmbH, Weil am Rhein, Germany; ArgGly obtained as a hydrochloride salt) were prepared at a concentration of 2 mM. Acetic acid was added (2.5 mM) to generate the protonated dipeptides, and metal hydroxide (for lithium, sodium, and potassium) or chloride (for cesium) was added (2–4 mM) to generate the corresponding metal-cationized dipeptides. Ions were introduced into the mass spectrometer using electrospray at an infusion rate of 10–15 μL/min. Stored waveform inverse Fourier transforms were used to isolate precursor ions, which were then irradiated for 2–4 s with tunable radiation from FELIX. The same irradiation time was used for each precursor complex, and the irradiation times were optimized to produce extensive but not complete fragmentation of the precursor at the frequency of maximum absorption. For ArgGly•Cs<sup>+</sup>, the region ~1450–1800 cm<sup>-1</sup> was rescanned with the laser attenuated by 3 dB to reduce peak broadening in this region due to saturation effects.

**Computations.** Low-energy structures for isolated and M<sup>+</sup>-complexed GlyArg and ArgGly were generated with Monte Carlo conformational searching using the MMFFs force field as implemented in *Macromodel 9.1* (Schrödinger, Inc., Portland, OR). To ensure that many possible combinations of arginine side chain, amide bond, and carboxylic acid conformations were sampled,

separate Monte Carlo searches beginning with different combinations of these conformations were performed, resulting in at least 40 000 structures for charge-solvated (CS) and salt bridge (SB) forms of each of the neutral, protonated, lithiated, and potassiumated dipeptides. The resulting low-energy structures were separated into families based on similarities in metal ion binding motif and dipeptide conformation. The geometries of representative structures from each of these families were optimized at the B3LYP/LACVP\* level of theory (Schrödinger, Inc., Portland, OR). LACVP\* is identical to the 6-31G\* basis set for all elements used in these computations except cesium, for which an effective core potential is used. Sodium and cesium cations were substituted into the representative lithiated and potassiumated starting structures, respectively, and geometries of the resulting sodiated and cesiated starting structures were optimized using B3LYP/LACVP\*.

All B3LYP/LACVP\* optimized structures were then optimized further in *Q-Chem v. 3.0*<sup>69</sup> using B3LYP/6-31+G(d,p) for all elements except cesium, for which the CRENL effective core potential and basis set were used. To determine the gas-phase proton affinities and basicities of the dipeptides, single-point energies were obtained using the B3LYP/6-31+G(d,p) optimized structures and B3LYP/6-311++G(2d,2p) and RI-LMP2/6-311++G(2d,2p)/aug-cc-PVTZ, RI-LMP2, or local Møller–Plesset second-order perturbation theory using the “resolution of the identity” approximation, which has been found to give electronic energies for peptides typically within 2 kJ/mol of full MP2.<sup>70</sup> Vibrational frequencies and intensities were calculated using the double harmonic approximation and the analytical (for neutral, protonated, lithiated, sodiated, and potassiumated species) or numerical Hessian (for cesiated species) of the B3LYP/6-31+G(d,p)/CRENL optimized structures.

Temperature and entropy corrections to the electronic energies of the complexes were determined using the unscaled B3LYP/6-31+G(d,p)/CRENL vibrational frequencies. These frequencies are scaled by 0.975 in the calculated spectra. This scaling factor has been found previously to give good agreement with experimental data for this and similar levels of theory.<sup>10,16–20,51</sup> Peak shapes are approximated in calculated spectra by convolution with a 30 cm<sup>-1</sup> fwhm Lorentzian distribution.

Absolute gas-phase proton affinities (PA<sub>298</sub> = -ΔH for protonation) and basicities at 298 K (GB<sub>298</sub> = -ΔG for protonation)<sup>71</sup> were calculated for the lowest-energy B3LYP/6-31+G(d,p) structure of GlyArg and all three lowest-energy structures of ArgGly. These values were obtained at the B3LYP/6-31+G(d,p), B3LYP/6-311++G(2d,2p)//6-31+G(d,p), and RI-LMP2/6-311++G(2d,2p)/aug-cc-PVTZ//B3LYP/6-31+G(d,p) levels of theory. The zero point energies, enthalpy, and temperature corrections used for these values were obtained using unscaled B3LYP/6-31+G(d,p) calculated frequencies.

## Results and Discussion

**IRMPD Spectra.** IRMPD spectra were obtained for ArgGly•M<sup>+</sup> (M = H, Li, Na, K, and Cs) and GlyArg•M<sup>+</sup> (M = H, Li, Na, and Cs) over the range ~900–1800 cm<sup>-1</sup>. An IRMPD yield was determined from the precursor (*I<sub>p</sub>*) intensity and the sum of the fragment ion intensities (*I<sub>f</sub>*) after laser irradiation at each frequency;

$$\text{IRMPD yield} = \left( \sum I_f \right) / \left( I_p + \sum I_f \right)$$

and this was normalized linearly with laser power to roughly account for the change in laser power as a function of photon energy.<sup>15</sup> The resulting IRMPD spectra are shown in Figure 1,

- (56) Fujihara, A.; Matsumoto, H.; Shibata, Y.; Ishikawa, H.; Fuke, K. *J. Phys. Chem. A* **2008**, *112*, 1457–1463.  
 (57) Lucas, B.; Grégoire, G.; Lemaire, J.; Maitre, P.; Glotin, F.; Schermann, J. P.; Desfrancois, C. *Int. J. Mass Spectrom.* **2005**, *243*, 105–113.  
 (58) Poffler, N. C.; Oomens, J.; Suhai, S.; Paizs, B. *J. Am. Chem. Soc.* **2007**, *129*, 5887–5897.  
 (59) Stearns, J. A.; Guidi, M.; Boyarkin, O. V.; Rizzo, T. R. *J. Chem. Phys.* **2007**, *127*, 154322.  
 (60) Vaden, T. D.; de Boer, T. S. J. A.; Simons, J. P.; Snoek, L. C. *Phys. Chem. Chem. Phys.* **2008**, *10*, 1443–1447.  
 (61) Vaden, T. D.; de Boer, T. S. J. A.; Simons, J. P.; Snoek, L. C.; Suhai, S.; Paizs, B. *J. Phys. Chem. A* **2008**, *112*, 4608–4616.  
 (62) Wong, C. H. S.; Ma, N. L.; Tsang, C. W. *Chem.—Eur. J.* **2002**, *8*, 4909–4918.  
 (63) Gross, D. S.; Williams, E. R. *J. Am. Chem. Soc.* **1996**, *118*, 202–204.  
 (64) Oh, H.; Breuker, K.; Sze, S. K.; Ge, Y.; Carpenter, B. K.; McLafferty, F. W. *Proc. Natl. Acad. Sci. U.S.A.* **2002**, *99*, 15863–15868.  
 (65) Shelimov, K. B.; Clemmer, D. E.; Hudgins, R. R.; Jarrold, M. F. *J. Am. Chem. Soc.* **1997**, *119*, 2240–2248.  
 (66) von Helden, G.; Wyttenbach, T.; Bowers, M. T. *Science* **1995**, *267*, 1483–1485.  
 (67) Wyttenbach, T.; von Helden, G.; Bowers, M. T. *J. Am. Chem. Soc.* **1996**, *118*, 8355–8364.  
 (68) Valle, J. J.; Eyler, J. R.; Oomens, J.; Moore, D. T.; van der Meer, A. F. G.; von Helden, G.; Meijer, G.; Hendrickson, C. L.; Marshall, A. G.; Blakney, G. T. *Rev. Sci. Instrum.* **2005**, *76*, 023103.

(69) Shao, Y.; et al. *Phys. Chem. Chem. Phys.* **2006**, *8*, 3172–3191.

(70) DiStasio, R. A.; Jung, Y.; Head-Gordon, M. *J. Chem. Theory Comput.* **2005**, *1*, 862–876.

(71) Zhang, K.; Chung-Phillips, A. *J. Phys. Chem. A* **1998**, *102*, 3625–3634.

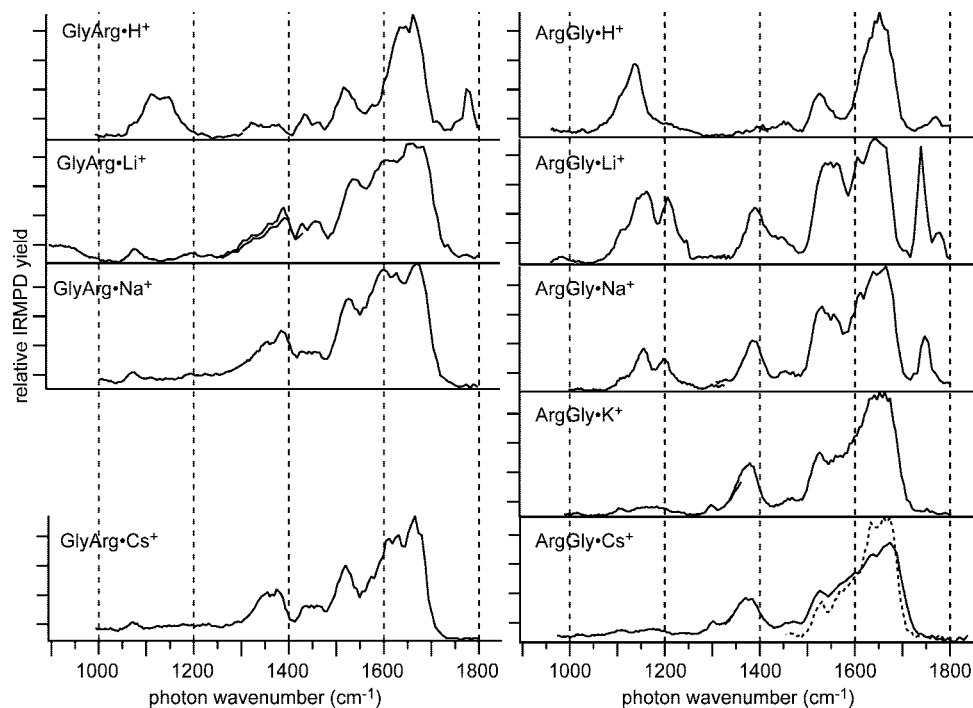


**Figure 1.** IRMPD spectra of protonated and alkali metal-cationized GlyArg and ArgGly. The dotted trace in the spectrum of ArgGly•Cs<sup>+</sup> is the relative IRMPD yield obtained with 3 dB attenuation of the laser.

**Table 1.** Precursor and Major Product Ion *m/z* Ratios and Ion Identifications where Possible<sup>a</sup>

complex studied	product ion <i>m/z</i>	assignment
ArgGly•H <sup>+</sup> ( <i>m/z</i> 232)	157	loss of glycine
	172	loss of 60 Da <sup>b</sup>
	215	–NH <sub>3</sub>
ArgGly•Li <sup>+</sup> ( <i>m/z</i> 238)	178	loss of 60 Da <sup>b</sup>
	220	–H <sub>2</sub> O
ArgGly•Na <sup>+</sup> ( <i>m/z</i> 254)	179	loss of glycine
	194	loss of 60 Da <sup>b</sup>
	236	–H <sub>2</sub> O
ArgGly•K <sup>+</sup> ( <i>m/z</i> 270)	39/41	K <sup>+</sup>
ArgGly•Cs <sup>+</sup> ( <i>m/z</i> 364)	133	Cs <sup>+</sup>
GlyArg•H <sup>+</sup> ( <i>m/z</i> 232)	157	loss of glycine
	158	loss of 74 Da <sup>b</sup>
	172	loss of 60 Da <sup>b</sup>
	214	–H <sub>2</sub> O
GlyArg•Li <sup>+</sup> ( <i>m/z</i> 238)	178	loss of 60 Da <sup>b</sup>
	220	–H <sub>2</sub> O
GlyArg•Na <sup>+</sup> ( <i>m/z</i> 254)	194	loss of 60 Da <sup>b</sup>
	236	–H <sub>2</sub> O
GlyArg•Cs <sup>+</sup> ( <i>m/z</i> 364)	133	Cs <sup>+</sup>

<sup>a</sup> Major product ions constitute at least 15% of the observed product ion population for a given complex. <sup>b</sup> Fragmentation products corresponding to the loss of 60 and 74 Da have been reported in collisionally induced dissociation mass spectra for cationized GlyArg and ArgGly and are discussed elsewhere.<sup>78</sup>

and major fragment ions (>15% of the fragment ion population) are listed in Table 1.

The IRMPD spectrum of GlyArg•H<sup>+</sup> is very similar to the previously reported spectrum of Arg•H<sup>+</sup>.<sup>21</sup> Specifically, bands similar in position and relative intensity to those assigned for Arg•H<sup>+</sup> to a free endo hydroxyl in-plane bend, overlapping NH bends, and a carboxylic acid carbonyl are present in the experimental spectrum of GlyArg•H<sup>+</sup> at 1100–1150 cm<sup>–1</sup>,

1600–1700 cm<sup>–1</sup>, and 1750–1780 cm<sup>–1</sup>, respectively. Two additional bands, a weak, broad feature from 1300–1400 cm<sup>–1</sup> and a sharp feature at ~1530 cm<sup>–1</sup>, are observed for GlyArg•H<sup>+</sup> that are not present in the spectrum of Arg•H<sup>+</sup>. The sharp feature at 1530 cm<sup>–1</sup> is consistent with the strong amide NH in-plane bend as observed for gas-phase *N*-methylacetamide,<sup>72</sup> which serves as a model for the carbonyl stretch and NH in-plane bend of an amide group in a dipeptide. Additionally, the intense band from 1600–1700 cm<sup>–1</sup> in the spectrum of GlyArg•H<sup>+</sup> is somewhat broader than its counterpart for Arg•H<sup>+</sup>, consistent with the added intensity of an amide carbonyl stretch in this region for GlyArg•H<sup>+</sup>. These results indicate that GlyArg•H<sup>+</sup> is protonated on the arginine side chain, and the C- and N-termini are formally neutral.

The spectra of ArgGly•H<sup>+</sup> and GlyArg•H<sup>+</sup> are very similar, suggesting that the major spectroscopic features identified above for GlyArg•H<sup>+</sup> depend little on the order of the residues in the dipeptide. Both an endo in-plane hydroxyl bend and a carboxylic acid carbonyl stretch, diagnostic of a nonzwitterionic structure, are clearly present in the spectrum of ArgGly•H<sup>+</sup>, although the carboxylic acid carbonyl stretch is relatively weak compared to that in the spectrum of GlyArg•H<sup>+</sup>. This difference may be due to a low-energy structure of ArgGly•H<sup>+</sup> that differs from the ground state primarily in the chemical environment of the carbonyl, e.g., an exo versus endo hydroxyl orientation for the carboxylic acid group. Absorption of a few photons could populate this transient structure, shifting the carbonyl stretch mode out of resonance with the laser and leading to a lower photodissociation yield at this frequency.

The spectra of GlyArg•M<sup>+</sup>, for M = Li, Na, and Cs, differ significantly from that of GlyArg•H<sup>+</sup> in that they contain neither a strong hydroxyl band near 1150 cm<sup>–1</sup> (or, indeed, any strong bands below 1300 cm<sup>–1</sup>) nor a carboxylic acid carbonyl stretch

(72) FT-IR spectrum obtained from NIST Webbook URL: <http://webbook.nist.gov/chemistry/>

above  $1700\text{ cm}^{-1}$ . Instead, much more relative photodissociation is observed for  $M = \text{Li, Na, and Cs}$  near  $1600\text{ cm}^{-1}$  and from  $1300\text{--}1400\text{ cm}^{-1}$ . The strong similarity of the spectra of the lithiated, sodiated, and cesiated forms of GlyArg suggests that these three complexes adopt nearly the same structure. The clear absence of carboxylic acid carbonyl stretches and hydroxyl in-plane bends as observed for GlyArg•H<sup>+</sup> indicates that GlyArg•M<sup>+</sup>,  $M = \text{Li, Na, and Cs}$ , form SB structures. Carboxylic acid carbonyl stretch bands have not been observed below  $1700\text{ cm}^{-1}$  in IRMPD spectra of other alkali metal-cationized amino acids or dipeptides. The carboxylate asymmetric stretching mode in metal-cationized amino acids and peptides falls below  $1700\text{ cm}^{-1}$  and presumably contributes to the relatively intense photodissociation near  $1600\text{ cm}^{-1}$ .

The spectra of lithiated and sodiated ArgGly contain a strong band in the same region as that of the endo hydroxyl in-plane bend of ArgGly•H<sup>+</sup> as well as a sharp, diagnostic carboxylic acid carbonyl stretch peak at  $1740$  and  $1748\text{ cm}^{-1}$  respectively for Li and Na. These results indicate the presence of CS forms of both ArgGly•Li<sup>+</sup> and ArgGly•Na<sup>+</sup>. The carboxylic acid carbonyl band for these two species is noticeably red-shifted from that of protonated ArgGly and is consistent with significant solvation of the metal ion by the carboxylic acid group, which should reduce the effective bond order of the carbonyl bond, thereby lowering the frequency of the associated carbonyl stretch. The charge density of the lithium cation is greater than that of the sodium cation, resulting in greater charge transfer to the solvating carboxylic acid carbonyl and a corresponding greater shift in this band position for the lithiated species. A shoulder band at  $\sim 1780\text{ cm}^{-1}$  is also present in the spectrum of ArgGly•Li<sup>+</sup>, suggesting the presence of a small population of conformers in which the carboxylic acid carbonyl does not solvate the charge and therefore has a stretching mode that is not significantly red-shifted. The spectra of both lithiated and sodiated ArgGly contain a much stronger amide NH in-plane bend feature than is observed for ArgGly•H<sup>+</sup>, as well as strong bands at  $\sim 1200$  and  $\sim 1380\text{ cm}^{-1}$ , neither of which is present in the spectrum of ArgGly•H<sup>+</sup>. These two new bands can be attributed to the symmetric and asymmetric coupling of two NH bending modes associated with a neutral guanidino group (vide infra).

The IRMPD spectra of ArgGly•K<sup>+</sup> and ArgGly•Cs<sup>+</sup> are strikingly similar to each other but differ significantly from those of ArgGly•H<sup>+</sup> and ArgGly•Li<sup>+</sup>. The absence of strong bands for both a hydroxyl in-plane bend and a carboxylic acid carbonyl stretch indicate that potassiumated and cesiated ArgGly form SB structures, consistent with increased intensity around  $1650\text{ cm}^{-1}$  compared to ArgGly•Li<sup>+</sup> attributable to a carboxylate asymmetric stretch. Weak, broad photodissociation between  $1100$  and  $1200\text{ cm}^{-1}$  is evident in the spectra of ArgGly•K<sup>+</sup> and ArgGly•Cs<sup>+</sup> but is attributable to many overlapping CH<sub>2</sub> bending modes as well as CC and CN stretching modes. Such a weak, broad feature is visible as a tail to the blue of the OH in-plane bend in the spectrum of ArgGly•H<sup>+</sup> and is likely buried beneath the much stronger features in the spectra of ArgGly•Li<sup>+</sup> and ArgGly•Na<sup>+</sup> in this region.

The features below  $1300$  and above  $1700\text{ cm}^{-1}$  in the spectrum of ArgGly•Na<sup>+</sup> are relatively less intense than for ArgGly•Li<sup>+</sup>, and the remaining bands correspond very well to the only intense features in the spectra of ArgGly•K<sup>+</sup> and ArgGly•Cs<sup>+</sup> over the region measured. Because the lesser degree of charge transfer to the carboxylic acid group from Na<sup>+</sup> as compared to Li<sup>+</sup> in an otherwise identical structure would be

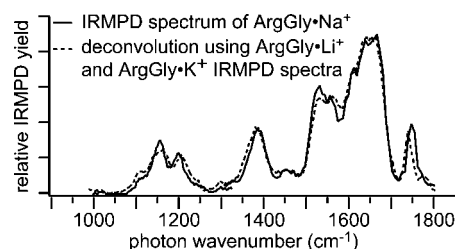


**Figure 2.** Deconvolution of the IRMPD spectrum of ArgGly•Na<sup>+</sup> using a 40:60 ratio of the IRMPD spectra of ArgGly•Li<sup>+</sup>/ArgGly•K<sup>+</sup>, normalized to their highest IRMPD yield.

expected to result in an *increased* relative intensity of the hydroxyl in-plane bend and carboxylic acid carbonyl stretch, it seems likely that a significant population of a second conformation of ArgGly•Na<sup>+</sup> must be present to explain the appearance of the spectrum. This second ion population is likely similar to the SB form of ArgGly•K<sup>+</sup> and ArgGly•Cs<sup>+</sup>. A crude deconvolution of the ArgGly•Na<sup>+</sup> experimental spectrum (Figure 2), obtained as a linear combination of the experimental spectra of ArgGly•Li<sup>+</sup> (representing a CS complex of ArgGly•M<sup>+</sup>) and ArgGly•K<sup>+</sup> (representing a SB complex of ArgGly•M<sup>+</sup>), normalized to their highest peak intensities, indicates that the ArgGly•Na<sup>+</sup> spectrum may possibly represent as much as a  $\sim 40\text{--}60\%$  population of SB conformers, as a very rough approximation. Because of different fragmentation efficiencies, the potential for interconversion between different structures, and other factors, it must be emphasized that such a deconvolution is only an approximation of the relative population of both structures. Interestingly, Arg•Na<sup>+</sup> was previously assigned to a roughly 90:10 mixture of structures similar to those identified for Arg•K<sup>+</sup> and Arg•Li<sup>+</sup>,<sup>22</sup> suggesting that the addition of a C-terminal glycyl group lessens the degree of preferential stabilization of the SB form of ArgGly•M<sup>+</sup> over the CS form compared to Arg•M<sup>+</sup>. Thus, despite the greater flexibility of ArgGly compared to Arg, which could potentially facilitate the formation of SB structures as appears to be the case for GlyArg, the strongly charge-solvating amide carbonyl group<sup>27,28,51</sup> competitively stabilizes the CS form of ArgGly.

**Dissociation by Loss of Small Neutral Molecules.** Fast heating of ions using UV radiation or slow heating by multiple consecutive collisions with gas-phase molecules or by multiple absorptions of infrared photons often leads to the loss of small molecules, such as H<sub>2</sub>O or NH<sub>3</sub>, from protonated or metal-cationized amino acids or peptides. Loss of such molecules has often been used to infer information about ionic structures. For example, loss of CO<sub>2</sub> upon activation of protonated peptides by  $157\text{ nm}$  photodissociation was used to infer the presence or absence of the SB form for peptides.<sup>73</sup> In our IRMPD experiments, loss of H<sub>2</sub>O but not NH<sub>3</sub> is observed for ArgGly•M<sup>+</sup> and GlyArg•M<sup>+</sup>,  $M = \text{Li and Na}$  (Table 1). GlyArg•M<sup>+</sup>,  $M = \text{Li and Na}$ , form SB structures, whereas ArgGly•Li<sup>+</sup> is a CS structure and ArgGly•Na<sup>+</sup> is a mixture of both forms. Thus, there is no direct relationship between the loss of a water molecule and whether the SB or CS form of these ions is more stable. Loss of H<sub>2</sub>O from the SB form of GlyArg•M<sup>+</sup>,  $M = \text{Li and Na}$ , requires that a proton and a hydrogen atom be transferred to the carboxylate group prior to dissociation. These results strongly indicate that the CS form is an intermediate in the dissociation pathway for loss of H<sub>2</sub>O from these two complexes, even though it is not populated in the ground state.

(73) Kjeldsen, F.; Silivra, O. A.; Zubarev, R. A. *Chem.—Eur. J.* **2006**, *12*, 7920–7928.

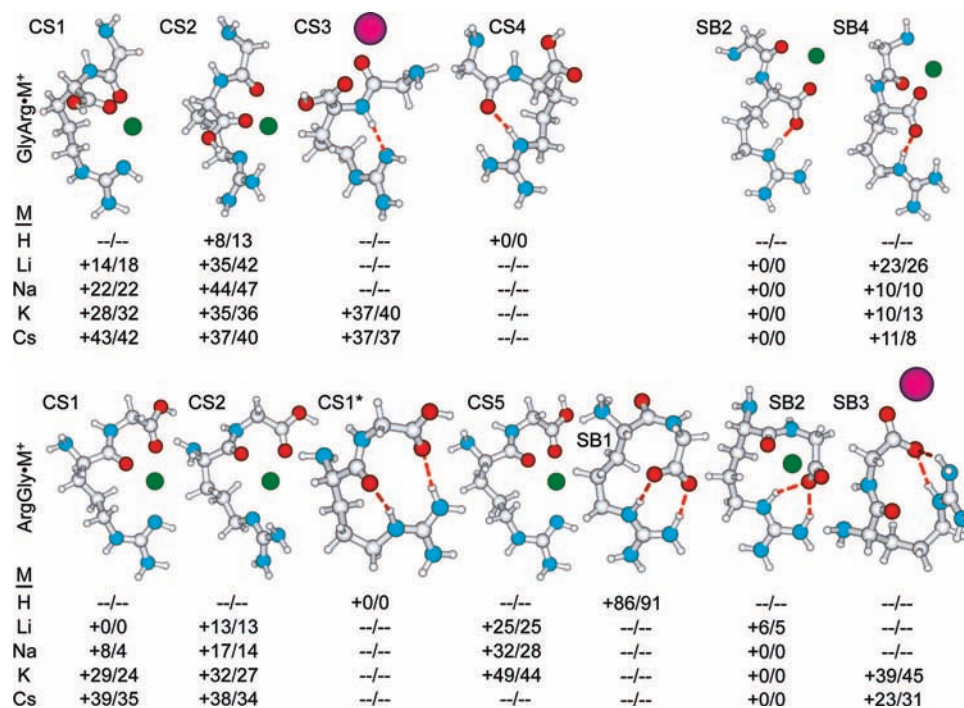


**Figure 3.** Low-energy structures and relative Gibbs free energies (kJ/mol) at 0/298 K for GlyArg•M<sup>+</sup> and ArgGly•M<sup>+</sup>. Structures for M = Na are shown except for GRM-CS4, RGM-CS1\*, and RGM-SB1, for which the protonated structure is shown, and GRM-CS3 and RGM-SB3, for which M = Cs is shown.

Similar results were obtained for Arg•M<sup>+</sup>, where the ratio of H<sub>2</sub>O loss to NH<sub>3</sub> loss changes as a function of metal cation size; H<sub>2</sub>O loss occurs exclusively for M = Li, whereas NH<sub>3</sub> loss but not H<sub>2</sub>O loss occurs for M = Rb and Cs.<sup>21,22,33</sup> This change in dissociation pathway with increasing cation size follows the trend in SB stability, but for Arg•Na<sup>+</sup>, the SB form is more stable, despite the predominant loss of H<sub>2</sub>O observed in both collisional activation experiments and IRMPD spectroscopy experiments in both the 800–1900 cm<sup>-1</sup> and 2600–3800 cm<sup>-1</sup> regions, indicating a CS form intermediate in both the collisional dissociation and IRMPD pathways.

Absorption of multiple photons is required to observe dissociation under the conditions of the experiments reported here, and precursor ions are irradiated by multiple macropulses from FELIX for 2–4 s. Thus, ion heating and dissociation can occur either within a single macropulse or more slowly over several macropulses in these experiments. An important question is the effect of slow heating on the observed IRMPD spectra, that is, whether these spectra reflect the ground-state structures of a thermal population of ions at the start of the experiment or whether higher-energy structures populated upon laser heating contribute. Because no absorption by the carboxylic acid carbonyl stretch is observed for SB structures of GlyArg•M<sup>+</sup>, M = Li and Na, despite loss of H<sub>2</sub>O, the higher energy CS intermediate does not contribute to the observed spectra. Previous studies have shown that band positions and intensities in IRMPD spectra can be quite similar to those of IR absorption spectra.<sup>74</sup> Although attendant uncertainties exist in comparing IRMPD spectra of a species with its linear IR absorption spectrum, the kinetic bottleneck in the IRMPD process is believed in most cases to be the absorption of the first few photons, so IRMPD spectra should often reflect the absorption

spectra of the precursor species.<sup>75</sup> The IRMPD spectra of these dipeptide complexes support photon absorption from the ground-state as being the rate-limiting step in dissociation and hence reflect the ground-state conformations. Less fidelity of the IRMPD spectrum to the absorption spectrum may potentially occur when minor rearrangement to transiently stable structures can occur early in the IRMPD process and shift vibrational modes significantly out of resonance with those of the ground state, as may be the case for the carboxylic acid carbonyl stretch of ArgGly•H<sup>+</sup>.

**Calculated Energies.** Because many different combinations are possible for the conformations of the peptide bond, N- and C-terminus, and arginine side chain, the conformational space for the monocationized dipeptides is very large and contains many local minima. Low-energy conformers with similar structures are grouped into structural families to simplify the identification of energetically competitive structure types that might contribute to the experimental spectra. The lowest-energy CS and SB structure families for each dipeptide complex, along with relative Gibbs free energies at 0 and 298 K, are shown in Figure 3. RG and GR designate ArgGly or GlyArg, respectively; M = H, Li, Na, K, or Cs; and CS<sub>n</sub> or SB<sub>n</sub> indicates “charge-solvated” or “salt bridge”, where *n* identifies the particular structural family. An asterisk indicates that the structure differs slightly from other structures with a similar alphanumeric designation.

A plot of the difference in Gibbs free energy at 0 and 298 K between the lowest-energy calculated CS and SB structures for each complex, Δ*G*<sub>SB-CS</sub>, as a function of metal ionic radius<sup>76</sup> (Table 2) is shown in Figure 4. The difference in Δ*G*<sub>SB-CS</sub> between ArgGly and GlyArg complexes of the same metal cation is greatest for lithium, where this value is ~20 kJ/mol,

(74) Oomens, J.; van Rooij, A. J. A.; Meijer, G.; von Helden, G. *Astrophys. J.* **2000**, *542*, 404–410.

(75) Oomens, J.; Sartakov, B. G.; Meijer, G.; von Helden, G. *Int. J. Mass Spectrom.* **2006**, *254*, 1–19.

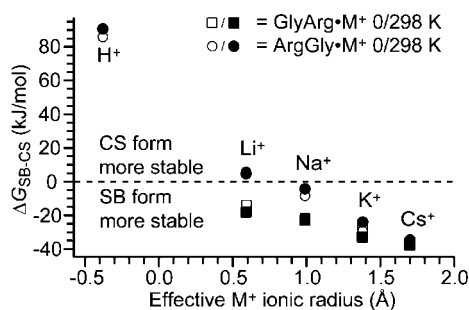


**Figure 4.**  $\Delta G_{\text{SB-CS}}$  for the lowest-energy SB and CS conformers of GlyArg•M<sup>+</sup> and ArgGly•M<sup>+</sup> at 0/298 K as a function of effective metal ionic radius.  $\Delta G_{\text{SB-CS}}$  was not calculated for GlyArg•H<sup>+</sup> because no stable low-energy SB structure was identified for this complex. Effective M<sup>+</sup> ionic radii are from ref 76.

and is smallest for cesium ( $\leq 3$  kJ/mol), indicating that relative stabilization of the SB form of these complexes over the CS form depends increasingly less on the order of the peptide residues with increasing metal ion size.

The B3LYP/6-31+G(d,p) energies are consistent with the assignments of the complexes as CS or SB structures based on the IRMPD spectra. For ArgGly•Na<sup>+</sup>, the lowest-energy CS structure is only 4 kJ/mol higher in Gibbs free energy at 298 K than the lowest-energy SB structure, so a significant proportion of CS structures would be expected in a Boltzmann population of ArgGly•Na<sup>+</sup> ions at room temperature.

**Low-Energy CS Structures.** The metal ion in the lowest-energy CS structures (CS1) for both dipeptides with Li, Na, and K is tricoordinate to the peptide carbonyl oxygen, carboxylic acid carbonyl oxygen, and side chain imine  $\eta$ -nitrogen. In these structures, the C-terminal carboxylic acid is in its endo orientation, and the hydroxyl group does not participate in solvating the charge, as reported for potassiumated PheAla and AlaPhe.<sup>51</sup> In general, a C-terminal hydroxyl group in an exo conformation is approximately 25 kJ/mol higher in energy for these complexes, in agreement with calculations for other cationized amino acid and peptide complexes.<sup>19,20,51</sup> The lone pair of the N-terminal nitrogen is oriented toward the amide NH group and participates in a weak hydrogen bond. This metal ion binding motif is analogous to that calculated previously for lithiated arginine,<sup>22</sup> except that coordination of the metal cation with the N-terminal nitrogen of arginine is substituted with coordination to the amide carbonyl of the dipeptide. The steric constraints of the peptide backbone render simultaneous coordination to both of these groups unfavorable, thereby making tetracoordination of the metal cation, reported to be lowest energy for singly hydrated metal-monocationized arginine,<sup>23</sup> unfavorable. Charge-solvation by the amide carbonyl oxygen atom is more effective than solvation by amine groups and carboxylic acid carbonyl oxygens.<sup>27,28,51</sup> Slightly different lowest-energy CS structures were found for ArgGly•Cs<sup>+</sup> and GlyArg•Cs<sup>+</sup>; a discussion of these and the lowest-energy protonated structures can be found in the Supporting Information.

**Low-Energy Calculated SB Structures.** All candidate SB structures identified for GlyArg•H<sup>+</sup> underwent proton transfer to give formally neutral N- and C-termini upon geometry optimization. In contrast, a stable SB structure, RGH-SB1, with a *cis*-amide bond was found for ArgGly•H<sup>+</sup>, but this structure is very high in energy (91 kJ/mol above RGH-CS1). The lowest-

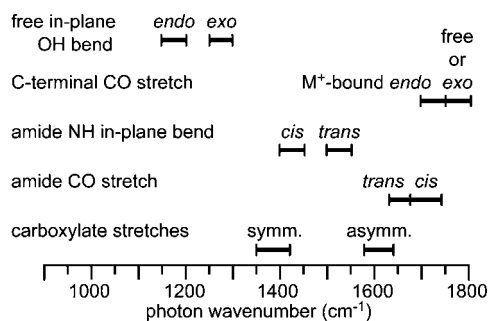


**Figure 5.** Expected regions of IR absorption for various conformations of strongly IR-active functional groups in GlyArg•M<sup>+</sup> and ArgGly•M<sup>+</sup> based on low-energy structures and frequencies calculated at the B3LYP/6-31+G(d,p)/CRENBL level of theory. All frequencies have been scaled by 0.975, which provides a reasonable fit to experimental data for these and similar complexes.

energy SB structures (SB2) for all of the alkali metal-cationized peptides are remarkably similar to each other in how they coordinate to the metal cation, but the order of the peptide residues induces a geometric constraint that has important energetic consequences. In the SB2 structures, the amide bond is in a *trans* conformation, and the metal ion is coordinated to the amide carbonyl oxygen and one carboxylate oxygen. For ArgGly•M<sup>+</sup>, the angle subtended by the formal charge carriers (the metal cation, the carboxylate carbon, and the central carbon of the guanidinium group) increases with metal ion size from 100° for Li to 112° for Cs. For GlyArg•M<sup>+</sup>, this angle is much larger and decreases with metal ion size from 173° for Li to 155° for Cs. Because the calculated lowest-energy CS structures for alkali metal-cationized ArgGly and GlyArg are similar, the greater relative stabilization of the lowest-energy SB structures for GlyArg versus ArgGly can be attributed primarily to the more favorable linear orientation of charge sites in the GlyArg SB complexes. The decreased dependence of  $\Delta G_{\text{SB-CS}}$  on peptide residue order with increasing metal cation size (vide supra) follows the convergence of the charge-site angle as a function of metal cation size, further underlining the importance of charge-site geometry on the stability of SB forms of these complexes. Further discussion of low-energy SB structures can be found in the Supporting Information.

**General Spectral Features.** On the basis of an analysis of the calculated spectra of the low-energy conformers identified for each complex, the spectral regions in which various group frequencies are expected to occur can be established (Figure 5). It should be noted that the carboxylate asymmetric stretch, which couples strongly to protonated arginine side chain NH bending modes between 1580 and 1640 cm<sup>-1</sup> in these calculations, is not expected to be easily identifiable as a single peak. Although SB or CS structures can be readily identified directly from the IRMPD spectra, comparisons between the measured spectra of these complexes and computed spectra provide more detailed structural information about the complexes. For each of the protonated and alkali metal-cationized complexes investigated, several low-energy structural families within 50 kJ/mol Gibbs free energy of the global minimum structure were identified. The most salient features in comparing experiment to theory are discussed below; all calculated structures, energies, and spectra are provided in the Supporting Information.

**GlyArg•H<sup>+</sup> and ArgGly•H<sup>+</sup>.** Figure 6 shows the experimental spectrum of GlyArg•H<sup>+</sup> along with three of the lowest-energy structures for this complex and their calculated spectra. The global minimum-energy structure, GRH-CS4, is a good fit to

(76) Shannon, R. D.; Prewitt, C. T. *Acta Crystallogr. B* **1969**, 25, 925–946.

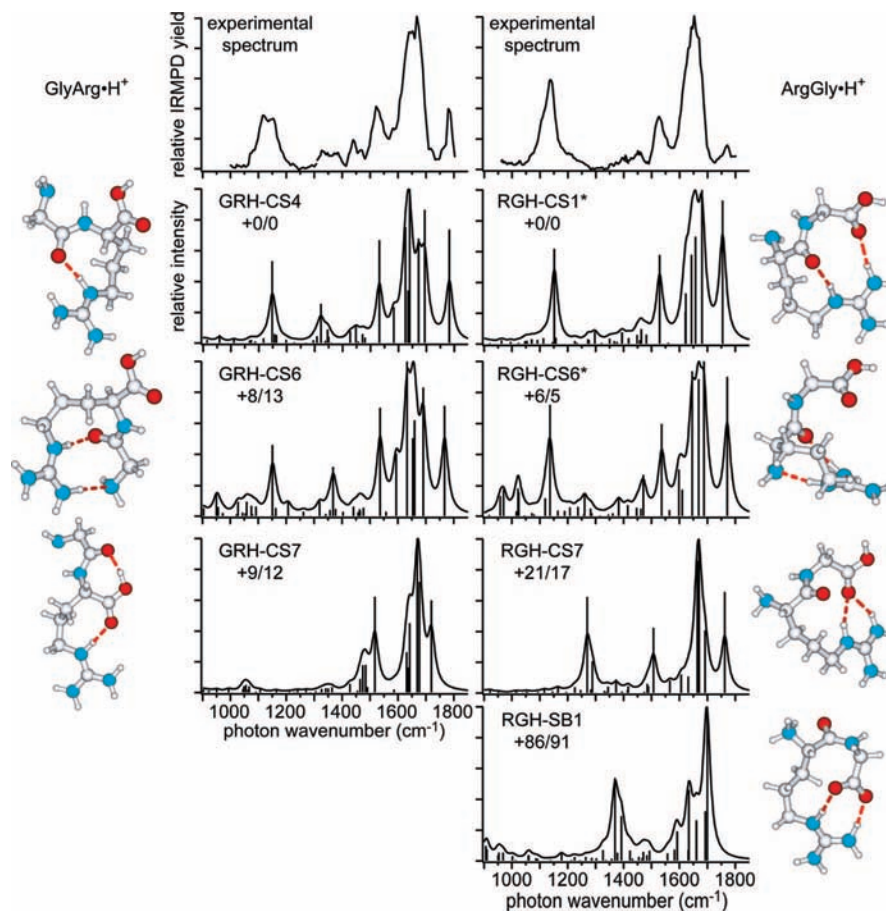


**Figure 6.** IRMPD spectra and low-energy structures and calculated spectra of GlyArg•H<sup>+</sup> and ArgGly•H<sup>+</sup>. Relative Gibbs free energies (kJ/mol) are reported at 0/298 K.

the experimental spectrum. Notably, the band predicted between 1300 and 1400 cm<sup>-1</sup> corresponds well to the experimental band in the same region and is attributable primarily to a CH bending mode of the arginyl  $\alpha$ -carbon (coupled to the carboxylic acid OH in-plane bend) and the CH<sub>2</sub> wag of the glycylic residue. The spectrum of structure GRH-CS6 is nearly identical to that of GRH-CS4, so both structures may contribute to the measured IRMPD spectrum. In contrast, the spectrum of structure GRH-CS7 has no band at  $\sim$ 1150 cm<sup>-1</sup>, and the charge-solvating carboxylic acid carbonyl stretch lies far to the red (1719 cm<sup>-1</sup>) of the experimental carboxylic acid carbonyl stretch at 1779 cm<sup>-1</sup>. It is therefore unlikely that GRH-CS7 contributes significantly to the measured IRMPD spectrum.

The calculated spectrum of the global minimum-energy structure RGH-CS1\* for ArgGly•H<sup>+</sup> fits the experimental spectrum quite well (Figure 6), differing primarily in the predicted intensity of the carboxylic acid carbonyl stretch. Another low-energy structure, RGH-CS6\*, is similar to GRH-CS6, except that the sites on the arginine side chain to which the N-terminal nitrogen and amide carbonyl oxygen are hydrogen-bonded are reversed. The calculated spectrum of this structure is also a reasonable spectroscopic fit to experiment, albeit not as good as that of RGH-CS1\*. A strong peak at  $\sim$ 1600 cm<sup>-1</sup> due to N-terminal amine and  $\eta$ -NH<sub>2</sub> scissoring modes is predicted for this structure but clearly has no counterpart in the experimental spectrum. A band at  $\sim$ 1020 cm<sup>-1</sup> due to the  $\epsilon$ -NH out-of-plane bend of the arginyl side chain is predicted for RGH-CS6\* but does not appear in the experimental spectrum, although the hydrogen atom in this group participates in a strong

hydrogen bond to the N-terminus, so that the calculated band position may not be reliable. Structures with an exo carboxylic acid hydroxyl group, such as RGH-CS7, are predicted to have hydroxyl in-plane bend modes far to the blue ( $>$ 1250 cm<sup>-1</sup>) of the one observed in the experimental spectrum and do not represent a substantial fraction of the experimental ion population. The calculated spectrum of RGH-SB1 is a very poor spectroscopic match to the experimental spectrum, and this structure likely does not contribute significantly to the measured IRMPD spectrum.

**GlyArg•M<sup>+</sup>.** The spectra of GlyArg•M<sup>+</sup>, M = Li, K, and Cs, are very similar to each other, although there are some subtle differences. Spectra for the three lowest-energy SB structures and the lowest-energy CS structure for M = Li and Cs are shown in Figure 7. Data for M = Na are very similar to those for Li (Supporting Information). The three strong bands calculated for GRLi-CS1 at 1160 cm<sup>-1</sup> (OH in-plane bend), 1214 cm<sup>-1</sup> (imine  $\eta$ -NH in-plane bend), and 1746 cm<sup>-1</sup> (carboxylic acid CO stretch) are clearly absent in the experimental spectra, indicating that this structure does not contribute significantly to the IRMPD spectrum of GlyArg•Li<sup>+</sup> (or GlyArg•Na<sup>+</sup>). The lowest-energy cesiated CS conformer, GRCs-CS3, can also be eliminated based on the intense calculated carboxylic acid carbonyl (1734 cm<sup>-1</sup>) and OH in-plane bend ( $\sim$ 1140 cm<sup>-1</sup>) that do not appear in the experimental spectrum.

The calculated band positions for the spectrum of the lowest-energy lithiated SB structure, GRLi-SB2, are a close match to the experimental spectrum, although the calculated relative intensities are different from those observed. In addition to the



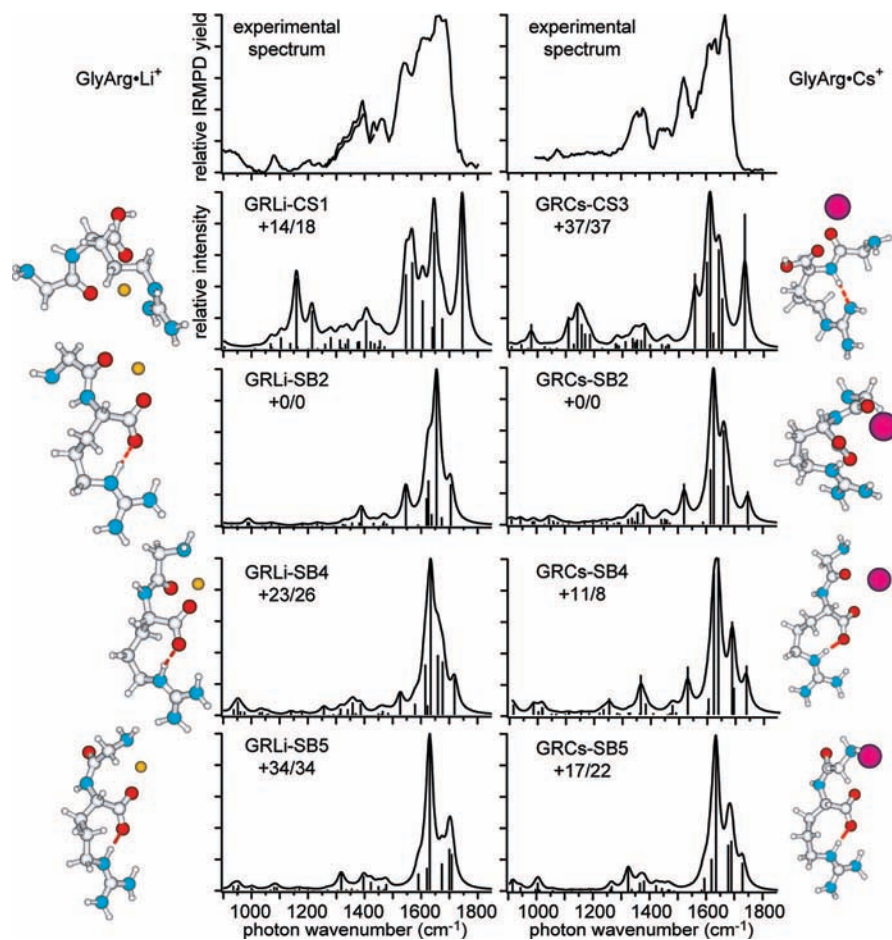


**Figure 7.** IRMPD spectra and low-energy structures and calculated spectra of  $\text{GlyArg}\cdot\text{Li}^+$  and  $\text{GlyArg}\cdot\text{Cs}^+$ . Relative Gibbs free energies (kJ/mol) are reported at 0/298 K.

already identified *trans*-amide NH in-plane bend at  $\sim 1540\text{ cm}^{-1}$  in the experimental spectrum, the calculated spectrum exhibits several dominant features close to major peaks in the experimental spectrum that aid in their identification. A carboxylate symmetric stretch is calculated to appear at  $\sim 1390\text{ cm}^{-1}$ , in good agreement with the experimental bands in this region, and two closely spaced bands from the carboxylate asymmetric stretch coupled with  $\eta$ -NH<sub>2</sub> scissoring motions calculated at  $\sim 1620$  and  $\sim 1630\text{ cm}^{-1}$  match well the experimental bands from  $1610$ – $1630\text{ cm}^{-1}$ . A strong amide carbonyl stretch at  $\sim 1655\text{ cm}^{-1}$  and a weaker  $\epsilon$ -NH in-plane bend at  $\sim 1710\text{ cm}^{-1}$  are predicted for GRLi-SB2 and are in satisfactory agreement with the observed intensity between  $1650$  and  $1700\text{ cm}^{-1}$  that peaks near  $1670\text{ cm}^{-1}$  for both complexes. Thus, SB2 is likely the dominant structure contributing to the experimental spectra of  $\text{GlyArg}\cdot\text{Li}^+$  and  $\text{GlyArg}\cdot\text{Na}^+$ .

Interestingly, the imine  $\epsilon$ -NH in-plane bend is predicted to be a weak band above  $1700\text{ cm}^{-1}$  in the spectra of GRM-SB2,  $M = \text{Li}, \text{Na}, \text{and Cs}$ , whereas virtually no photodissociation occurs in this spectral region. The strong, ionic hydrogen bond shared between this imine NH and the carboxylate group may result in significant anharmonicity in this mode, which is not accounted for by the double harmonic approximation used in these calculations. A similar discrepancy is present for the spectra of structures GRM-SB4, which otherwise match experiment quite well and may contribute to the ion population. It is possible that other structures not identified in the conformational search contribute to the experimental spectra. The higher-energy

SB structures GRM-SB5, in which a *cis*-amide group is present and the N-terminal nitrogen coordinates the metal cation instead of the amide carbonyl, have no bands near  $\sim 1540\text{ cm}^{-1}$ , where a strong band is observed in the experimental spectra. GRM-SB5 is therefore unlikely to form a significant portion of the experimental ion population for any of the metal cations studied.

**ArgGly•M<sup>+</sup>.** The experimental spectra of  $\text{ArgGly}\cdot\text{M}^+$ ,  $M = \text{Li}, \text{Na}, \text{K}, \text{and Cs}$ , clearly indicate a change from a CS structure to a SB structure with increasing metal ion size. The spectrum of the lowest-energy structure of  $\text{ArgGly}\cdot\text{Li}^+$ , RGLi-CS1, is a good fit to the experimental spectrum (Figure 8). The arginine  $\alpha$ -CH bending mode at  $\sim 1315\text{ cm}^{-1}$  calculated for these structures is not observed as a distinct peak in the experimental spectra, but photodissociation does occur in this region. In the sodiated complex, the carboxylic acid carbonyl stretch is red-shifted by 8 and  $6\text{ cm}^{-1}$  in the measured and calculated CS1 structures, respectively. Sharp bands are calculated near  $1200$  and  $1400\text{ cm}^{-1}$  for the symmetric and asymmetric coupling of the  $\epsilon$ -NH and imine  $\eta$ -NH in-plane bending modes of the arginyl side chain, and these correspond well in position and intensity to the experimental peaks in these regions for both  $\text{ArgGly}\cdot\text{Li}^+$  and  $\text{ArgGly}\cdot\text{Na}^+$ . Only one band is predicted in the  $1150$ – $1200\text{ cm}^{-1}$  region for the similar RGLi-CS2 structure, and no peaks are predicted between  $1550$  and  $1600\text{ cm}^{-1}$ , indicating that the CS2 structure does not contribute significantly to the measured spectra of  $\text{ArgGly}\cdot\text{Li}^+$  and  $\text{ArgGly}\cdot\text{Na}^+$ . The carbonyl stretch of the exo carboxylic acid group in structure RGLi-CS5 is calculated to appear at  $1766\text{ cm}^{-1}$ , much closer to the small

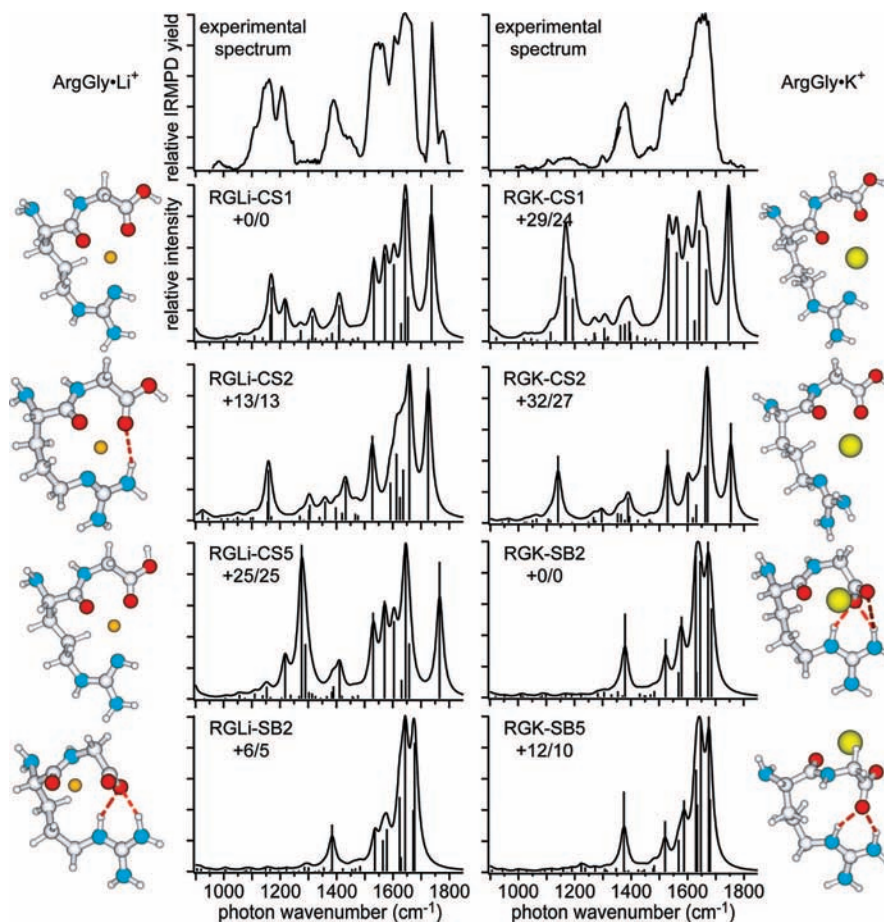


**Figure 8.** IRMPD spectra and low-energy structures and calculated spectra of ArgGly•Li<sup>+</sup> and ArgGly•K<sup>+</sup>. Relative Gibbs free energies (kJ/mol) are reported at 0/298 K.

peak at 1779 cm<sup>-1</sup> in the experimental spectrum than the predicted 1737 cm<sup>-1</sup> peak for the CS1 structure. Thus, structures with an exo carboxylic acid group may be present.

The spectrum of the lowest-energy SB structure calculated for ArgGly•Li<sup>+</sup>, RGLi-SB2, which is energetically competitive with the CS1 structure, contains bands corresponding to those in the experimental spectrum between 1350 and 1700 cm<sup>-1</sup>. The relative peak intensities match better for the sodiated species (Supporting Information). Thus, it is possible that a small population of SB2 could be present for ArgGly•Li<sup>+</sup>, and a larger population could be present for ArgGly•Na<sup>+</sup>.

The match between the IRMPD spectra of ArgGly•K<sup>+</sup> and ArgGly•Cs<sup>+</sup> and calculated spectra of their lowest-energy SB structures (RGK-SB2 and RGCs-SB2) is much better than that for any of the SB structures of GlyArg•M<sup>+</sup>, and these spectra are an excellent fit to the corresponding IRMPD spectra (data for ArgGly•K<sup>+</sup> shown in Figure 8). The only other low-energy structure family that matches well the experimental peaks at ~1375 cm<sup>-1</sup>, ~1530 cm<sup>-1</sup>, and 1550–1700 cm<sup>-1</sup> for both complexes is SB5, which is structurally very similar to SB2 and may also contribute to the experimental spectra. The calculated spectrum of the much higher-energy SB structure RGCs-SB3 for ArgGly•Cs<sup>+</sup> (Supporting Information), is a reasonable fit to experiment, although the relative intensity observed between 1550 and 1650 cm<sup>-1</sup> in the IRMPD spectrum is predicted better by structures SB2 and SB5.

**Effects of Gas-Phase Proton Affinity and Basicity.** The basicity of an amino acid can influence the relative energies of

**Table 2.** Gibbs Free Energy Differences in kJ/mol between the Lowest Energy SB and CS forms of GlyArg•M<sup>+</sup> and ArgGly•M<sup>+</sup>, M = H, Li, Na, K, and Cs, at 0 K/298 K, Obtained from B3LYP/6-31+G(d,p)/CRENBL Calculations; Positive  $\Delta G_{\text{SB-CS}}$  Values Indicate that the Lowest-Energy CS Form is More Stable than the Lowest-Energy SB Form

M	GlyArg•M <sup>+</sup> $\Delta G_{\text{SB-CS}}$	ArgGly•M <sup>+</sup> $\Delta G_{\text{SB-CS}}$
H	--/-- <sup>a</sup>	+86/+91
Li	-14/-18	+6/+5
Na	-22/-22	-8/-4
K	-28/-32	-29/-24
Cs	-37/-37	-38/-34

<sup>a</sup>  $\Delta G_{\text{SB-CS}}$  was not calculated for GlyArg•H<sup>+</sup> because no stable low-energy SB structure was identified for this complex.

its CS and SB forms, but this relationship for amino acids with side chain heteroatoms can be indirect.<sup>16–23</sup> To determine whether the intrinsic basicity of these two dipeptides is a factor in the relative stabilization of the SB form, the gas-phase proton affinities and basicities of these two dipeptides were calculated using several levels of theory (Table 3). The lowest-energy forms of neutral ArgGly and GlyArg are nonzwitterionic in their ground state at 0 and 298 K (Figure 9). The structure of GlyArg is similar to that of GlyArg•H<sup>+</sup>. For ArgGly, two structures are essentially isoenergetic with the global minimum structure, including a zwitterionic structure that resembles the lowest-energy form RGH-CS1 of ArgGly•H<sup>+</sup>.

The gas-phase proton affinity and basicity of ArgGly are consistently higher than those of GlyArg for all three levels of theory by > 10 kJ/mol and 2–6 kJ/mol, respectively. In contrast,

**Table 3.** Gas-Phase Proton Affinities ( $PA_{298}$ ) and Basicities ( $GB_{298}$ ) in kJ/mol at 298 K Calculated for GlyArg and ArgGly; Enthalpy and Entropy Corrections to the Electronic Energies Were Obtained from B3LYP/6-31+G(d,p) Frequency Calculations for all Levels of Theory

	level of theory/basis set	$PA_{298}$	$GB_{298}$
GlyArg	B3LYP/6-31+G(d,p)	1052	1029
	B3LYP/6-311++G(2d,2p)	1049	1027
	RI-LMP2/6-311++G(2d,2p)/aug-cc-PVTZ	1037	1014
ArgGly	B3LYP/6-31+G(d,p)	1067	1036
	B3LYP/6-311++G(2d,2p)	1066	1033
	RI-LMP2/6-311++G(2d,2p)/aug-cc-PVTZ	1047	1016

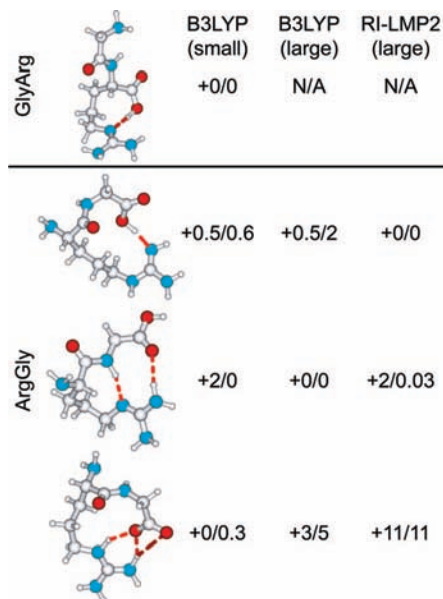


**Figure 9.** Lowest-energy structures and relative Gibbs free energies (kJ/mol) at 0/298 K calculated for GlyArg and ArgGly, using electronic energies calculated at the B3LYP and RI-LMP2 levels of theory using the 6-31+G(d,p) (“small”) and 6-311++G(2d,2p) (“large”) basis sets. aug-cc-PVTZ was the auxiliary basis for the RI-LMP2 calculations, and entropy and enthalpy corrections for all calculations were obtained from B3LYP/6-31+G(d,p) frequency calculations.

experimental results for ValXxx and XxxVal, indicate that the gas-phase basicity is often slightly higher when the more basic residue is C-terminal.<sup>77</sup> Results from the IRMPD spectroscopy experiments clearly indicate that alkali metal-cationized GlyArg has a greater tendency to adopt an SB structure than does ArgGly. Thus, the calculated proton affinity and basicity values are weakly anti-correlated to stabilization of the SB complexes. This indicates that, instead of dipeptide basicity, the dominant factor in the greater stability of GlyArg•M<sup>+</sup> SB complexes over those of ArgGly•M<sup>+</sup> is the ability of the GlyArg•M<sup>+</sup> SB complexes to adopt a more electrostatically favorable quasi-linear arrangement of formal charge sites than is possible for ArgGly•M<sup>+</sup> SB complexes.

(77) Gorman, G. S.; Amster, I. J. *J. Am. Chem. Soc.* **1993**, *115*, 5729–5735.

(78) Forbes, M. W.; Jockusch, R. A.; Young, A. B.; Harrison, A. G. *J. Am. Soc. Mass Spectrom.* **2007**, *18*, 1959–1966.

## Conclusions

Results from IRMPD spectroscopy clearly show that the sequence of the dipeptides containing Arg and Gly is important in the relative stabilities of the CS and SB forms when cationized by an alkali metal ion. ArgGly•Li<sup>+</sup> forms a CS structure, whereas ArgGly•M<sup>+</sup>, M = K and Cs, and GlyArg•M<sup>+</sup>, M = Li, Na, and Cs, form SB structures. For ArgGly•Na<sup>+</sup>, a roughly equal mixture of CS and SB structures is present. On the basis of these results, GlyArg•M<sup>+</sup>, M = K and Rb, and ArgGly•Rb<sup>+</sup> are expected to adopt SB structures. By comparison to previous results for Arg•M<sup>+</sup>, GlyArg•M<sup>+</sup> has a greater propensity to form SB structures, whereas that for ArgGly•M<sup>+</sup> is slightly lower. The difference in SB stabilities between these two dipeptides can be directly related to a conformational effect where GlyArg•M<sup>+</sup> can adopt a more linear arrangement of formal charge sites in the SB form. ArgGly is calculated to be slightly more basic than GlyArg, indicating that the intrinsic basicity of the peptide does not influence the stability of the SB form. These results suggest that SB structures should be common in larger protonated and metal-cationized peptides containing arginine, which are able to fold to form an optimal, quasi-linear arrangement of formal charge sites that favors the SB form. Additional studies on larger arginine-containing peptides will be useful for determining the role of the amide carbonyl oxygen atoms in competitively stabilizing the CS form. Results from computational chemistry of different structures show spectral regions where characteristic frequencies occur and should be useful for deducing structural information from the IRMPD spectra of much larger peptides where detailed comparisons to calculated spectra will be more difficult.

For several of the complexes that adopt SB structures, loss of a neutral water molecule is observed upon IRMPD. Loss of a water molecule from these ions must come about from a rearrangement involving a CS intermediate. The absence of a carboxylic acid carbonyl stretch in these spectra clearly indicates that the CS intermediate does not contribute to the IRMPD spectra. This shows that these spectra reflect the ground-state structures of these ions despite the multiple photon absorption required to observe fragmentation. These results also demonstrate that structural information about stable SB or CS structures inferred solely from observations of the loss of small neutral molecules can be misleading.

**Acknowledgment.** IRMPD spectra were acquired at the FOM Institute for Plasma Physics “Rijnhuizen”, which is financially supported by the Nederlandse Organisatie voor Wetenschappelijk Onderzoek (NWO). The authors thank Drs. Britta Redlich, Jeffrey D. Steill, and the rest of the FELIX staff for excellent support and Drs. Matthew F. Bush, Kathleen A. Durkin, and Jamin L. Krinsky for helpful conversations. Generous financial support was provided by the National Science Foundation (Grants CHE-0718790 and OISE-0730072).

**Supporting Information Available:** Full citation for reference 69 and all calculated structures, energies, and spectra. This material is available free of charge via the Internet at <http://pubs.acs.org>.

JA808177Z